Data Report: X-Ray Diffraction of Sediments from Green Canyon Block 955, Gulf of Mexico[1]

R. Heber, The Ohio State University, School of Earth Sciences, Columbus, Ohio, 43210

A. Cook, The Ohio State University, School of Earth Sciences, Columbus, Ohio, 43210

J. Sheets, The Ohio State University, School of Earth Sciences, Columbus, Ohio, 43210

D. Sawyer, The Ohio State University, School of Earth Sciences, Columbus, Ohio, 43210

1. Abstract

We performed 18 X-ray diffraction (XRD) measurements on sediment samples acquired at Holes H002 (6 samples) and H005 (12 samples) during the UT-GOM2-1 Expedition in Green Canyon Block 955, in the northern Gulf of Mexico. Results indicate a predominance of quartz, with significant proportions of alkali feldspar and carbonate, and minor amounts of amphibole, micas, and clays.

2. Introduction

The objective of this report is to present data and results of x-ray diffraction analysis on samples collected during the UT-GOM2-1 Expedition (Flemings et al., 2018). XRD is critical for mineral identification (Moore and Reynolds, 1989).

The UT-GOM2-1 Expedition in May, 2017 drilled two holes in Green Canyon Block 955 (GC 955) in the deepwater Gulf of Mexico: Hole GC 955 H002 (H002) and Hole GC 955 H005 (H005). 21 10 ft (3.05 m) pressure cores were attempted in, and near, the methane hydrate reservoir. In the first hole, H002, 1 of the 8 cores was recovered under pressure with 34% recovery of sediment (both pressurized and depressurized). In the second hole, H005, 12 of the 13 cores were recovered under pressure with 72% recovery of sediment. The pressure cores were imaged and logged under pressure.

[1]Heber, R., Cook, A., Sheets, J., and Sawyer, D., 2020. Data Report: X-Ray Diffraction of Sediments from Green Canyon Block 955, Gulf of Mexico. In Flemings, P.B., Phillips, S.C, Collett, T., Cook, A., Boswell, R., and the UT-GOM2-1 Expedition Scientists, Proceedings of the UT-GOM2-1 Hydrate Pressure Coring Expedition: Austin, TX (University of Texas Institute for Geophysics, TX). 27 p.

Initial receipt: 26 Sept 2019
Acceptance: 08 October 2019
Publication: 10 April 2020
Corresponding Author: Ann Cook cook.1129@osu.edu
Volume: https://dx.doi.org/10.2172/1646019
https://ig.utexas.edu/energy/genesis-of-methane-hydrate-in-coarse-grained-systems/expedition-ut-gom2-1/reports/

Depressurized sediment analyzed were either from pressure cores that were not recovered under pressure or from pressure cores quantitatively degassed either on-board or on-shore to determine the hydrate concentration and the gas composition. To document XRD, we used a PANalytical X'pert Pro X-ray diffractometer.

3. Methods and Materials

We performed X-ray diffraction measurements on a total of 18 samples (Table 1 and Table 2) using a PANalytical X'pert Pro X-ray diffractometer to determine the bulk mineralogy. 10 samples were sampled at Ohio State directly from cores. (Table 1). 8 samples were sent to Ohio State after initial sampling at UT-Austin (Table 2).

We followed standard protocol for sample preparation including drying and grinding 2 grams of sediment into a fine powder with a corundum mortar and pestle, and back-loading it into the bottom of a stainless steel cavity sample mount. Cu K-alpha radiation with a wavelength of 0.15418 nm was the incident radiation directed at the sample, and the diffracted (reflected) intensities off crystal planes were measured. The subsequent data were processed with the analytical software platform Highscore Plus along with the PDF 4+ mineral database in order to identify the minerals present based on diffraction peak patterns from the database.

We applied a Rietveld Method on five subsamples (Table 1 and Figures 19-25) to convert observed and calculated peak intensities into mineral weight percentages in order to provide a semi-quantitative estimate of mineral abundance. The Rietveld method models the full experimental pattern with a least squares residual approach (Rietveld, 1969).

For more information regarding cores, lithostratigraphy, and core photos, the reader is referred to the following archives:

H002: http://www-udc.ig.utexas.edu/gom2/H002/6_Lithostratigraphy/

H005: http://www-udc.ig.utexas.edu/gom2/H005/6_Lithostratigraphy/

4. Results

The results of the 18 bulk XRD measurements are shown graphically in Figures 1-18. The digital data for H002 are available here: http://www-udc.ig.utexas.edu/gom2/H002/6_Lithostratigraphy/XRD/ and for H005 here: http://www-udc.ig.utexas.edu/gom2/H005/6_Lithostratigraphy/XRD/

The XRD bulk mineral results indicate the predominance of quartz, with significant proportions of alkali feldspar and carbonate, and minor amounts of amphibole, micas, and clays. Semi-quantitative results from Rietveld refinement reveal a predominantly quartz based sediment with significant quantities of feldspars and carbonate, and minor quantities of micas, amphiboles, and clays (Figures 9-23). Quartz was the largest percentage in each subsample (24.0–46.8%), followed by albite (17.1–25.8%). Carbonates (calcite and dolomite) combined for a range of 13.3–24.3% across samples. Micas, both muscovite and biotite, made up 2.2–10.1%. Amphiboles accounted for 2–5.4%. Lastly, clay minerals including vermiculite, kaolinite and chlorite contributed 1.2–11%. Due to limitations inherent to

quantitative analysis, quartz, despite being the most abundant, was underestimated by the model (Figure 24), and albite, a feldspar mineral, was overestimated (Figure 25).

Subsamples with the highest quartz content came from the section of the reservoir with the highest hydrate saturation (sandy silt). Subsamples with the highest clay content came from the section of the reservoir with the lowest hydrate saturation (silty clay). Clayey silt illustrated a transition between these two endmembers of mineral abundance with a combination of quartz and clay and a moderate hydrate saturation.

Acknowledgements

XRD scans were acquired at the Subsurface Energy Materials Characterization and Analysis Laboratory (SEMCAL), School of Earth Sciences, The Ohio State University.

This work and the UT-GOM2-1 Hydrate Pressure Coring Expedition was funded by the Department of Energy Award DE-FE0023919, which is advised by the United States Geological Survey (USGS) and the Bureau of Ocean Energy Management (BOEM).

5. References

Flemings, P.B., Phillips, S.C, Collett, T., Cook, A., Boswell, R., and the UT-GOM2-1 Expedition Scientists, 2018. UT-GOM2-1 Hydrate Pressure Coring Expedition Summary. In Flemings, P.B., Phillips, S.C, Collett, T., Cook, A., Boswell, R., and the UT-GOM2-1 Expedition Scientists, Proceedings of the UT-GOM2-1 Hydrate Pressure Coring Expedition, Austin, TX (University of Texas Institute for Geophysics, TX). http://dx.doi.org/10.2172/1647223.

Flemings, P.B., Phillips, S.C, Collett, T., Cook, A., Boswell, R., and the UT-GOM2-1 Expedition Scientists, 2018, UT-GOM2-1 Hydrate Pressure Coring Expedition Data Directory, http://www-udc.ig.utexas.edu/gom2/.

Moore, D.M. and Reynolds Jr., R.C. (1989) X-Ray Diffraction and the Identification and Analysis of Clay Minerals. Oxford University Press, Oxford, p. 179-201.

Rietveld, H., 1969, A profile refinement method for nuclear and magnetic structures: Journal of Applied Crystallography, v. 2, p. 65-71.

6. Figures

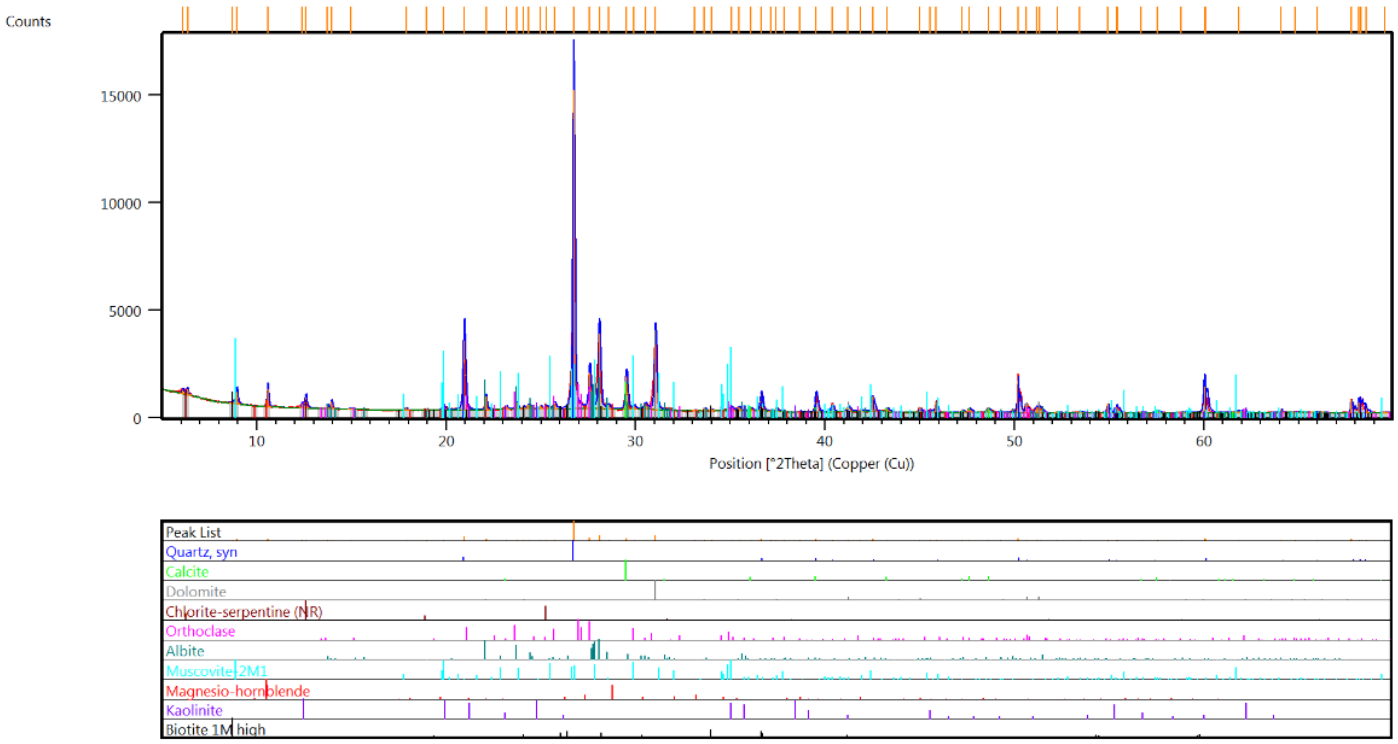

Figure 1. H002-2CS-1 phase ID.

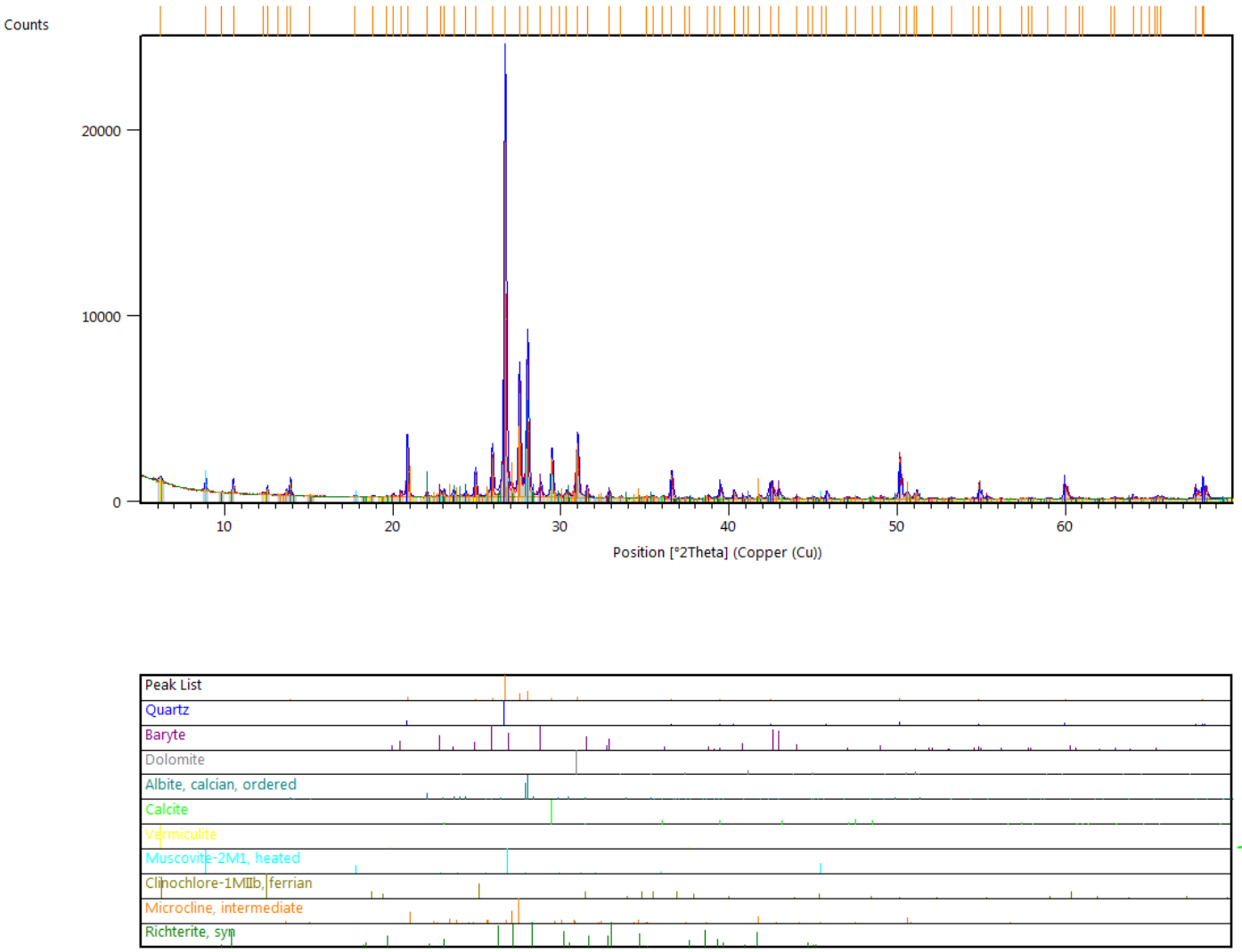

Figure 2. H002-3CS-1 phase ID (vermiculite is yellow).

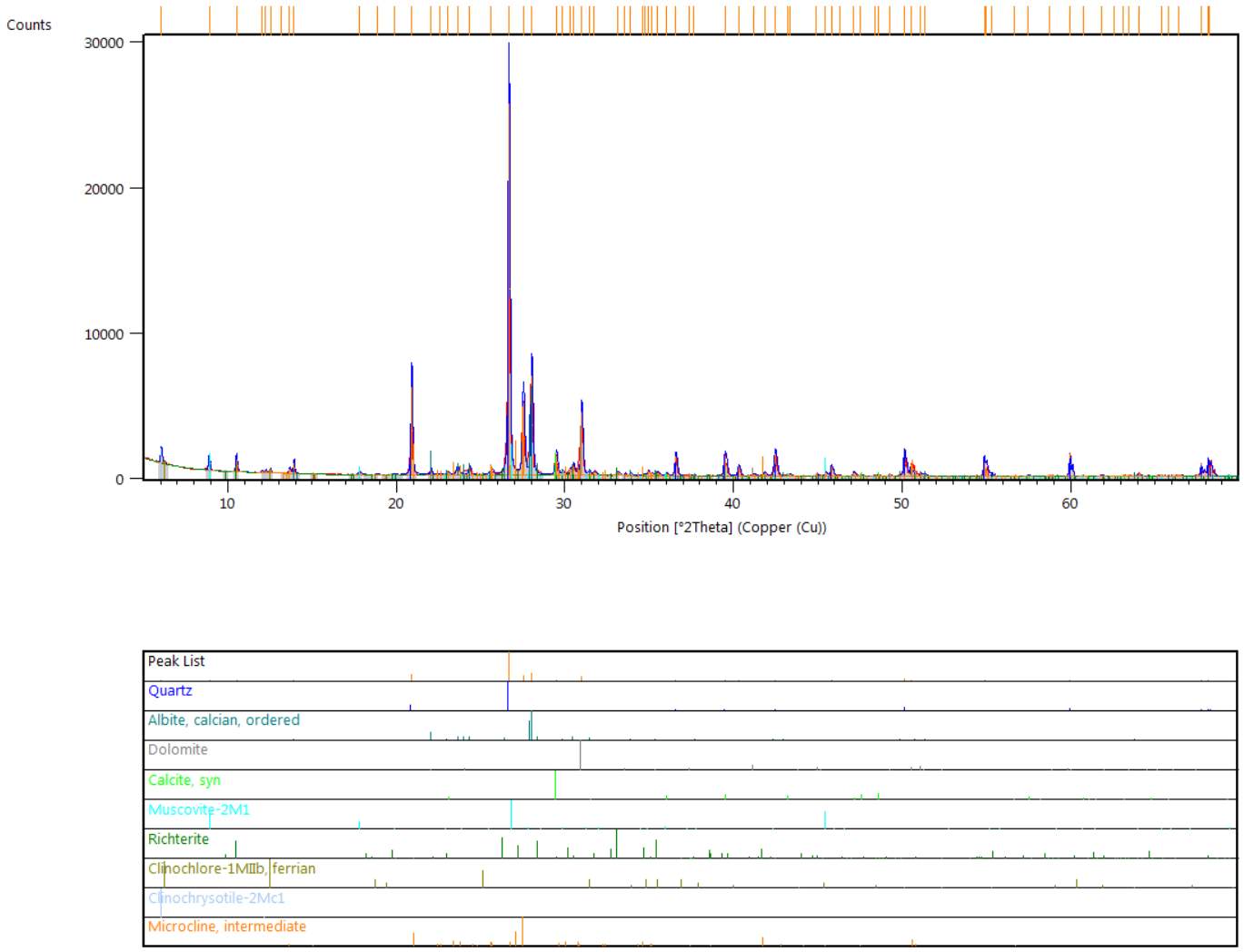

Figure 3. H002-3CS-1 phase ID.

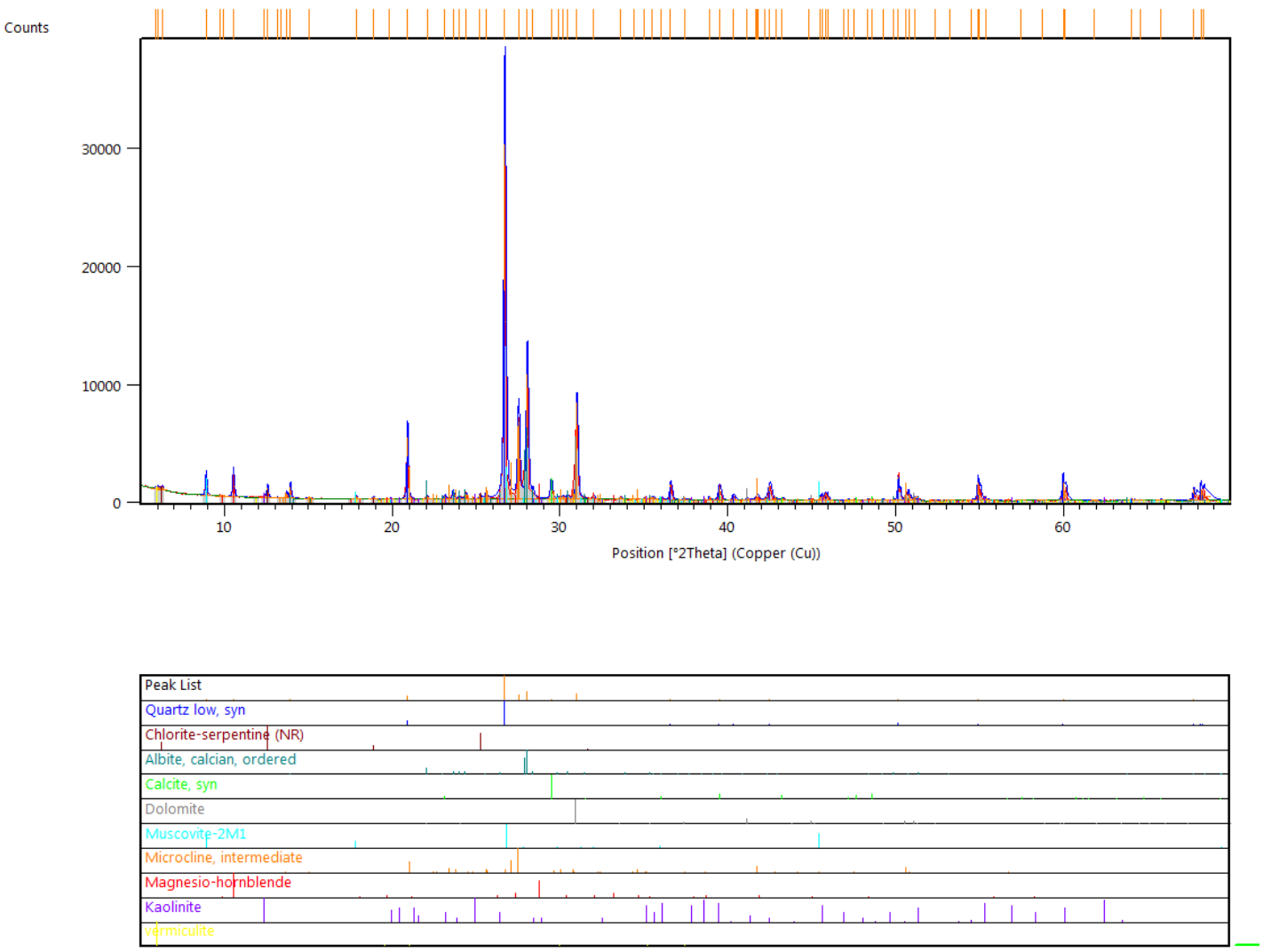

Figure 4. H002-6CS-3 phase ID (vermiculite is yellow).

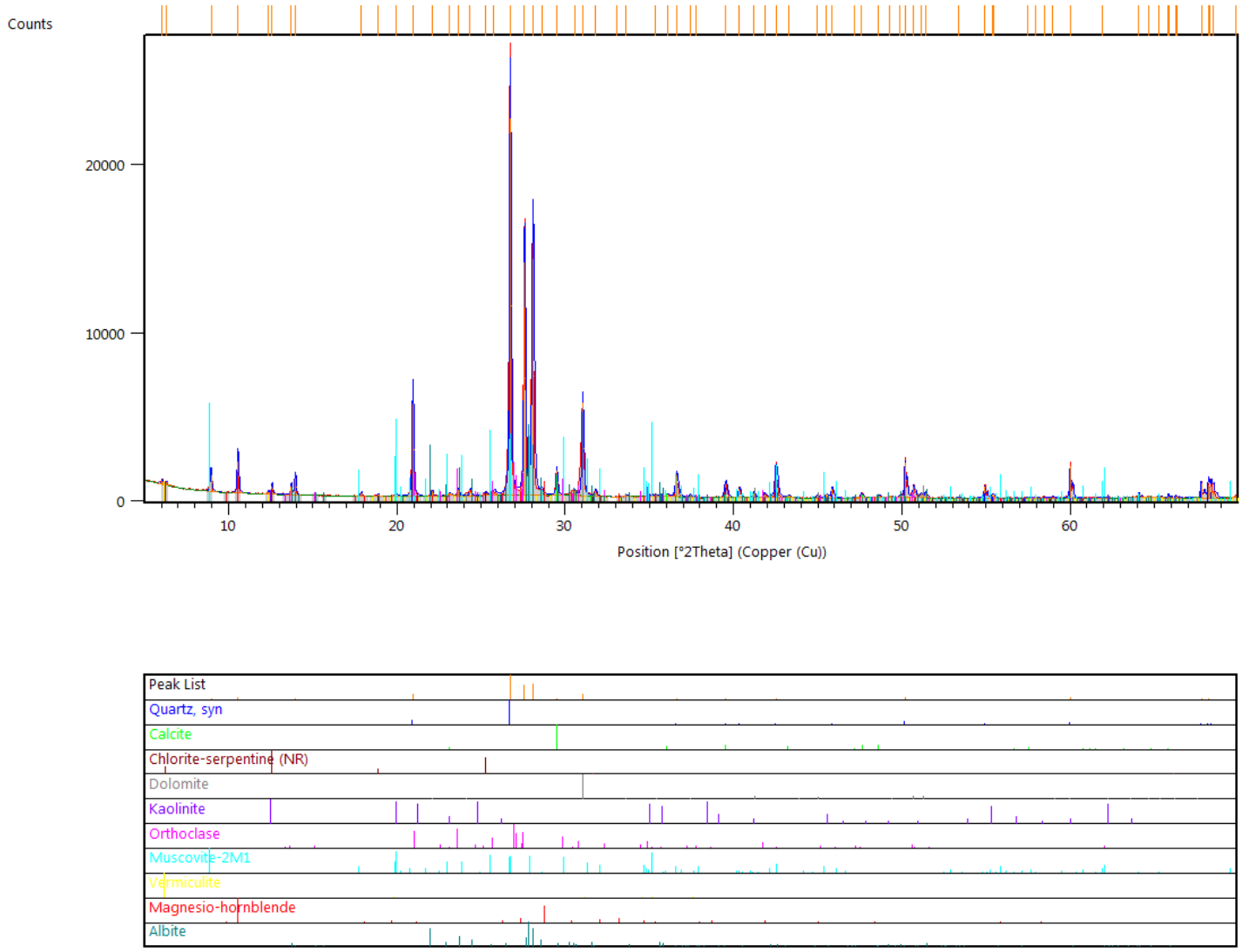

Figure 5. H002-7CS-1 phase ID (vermiculite is yellow).

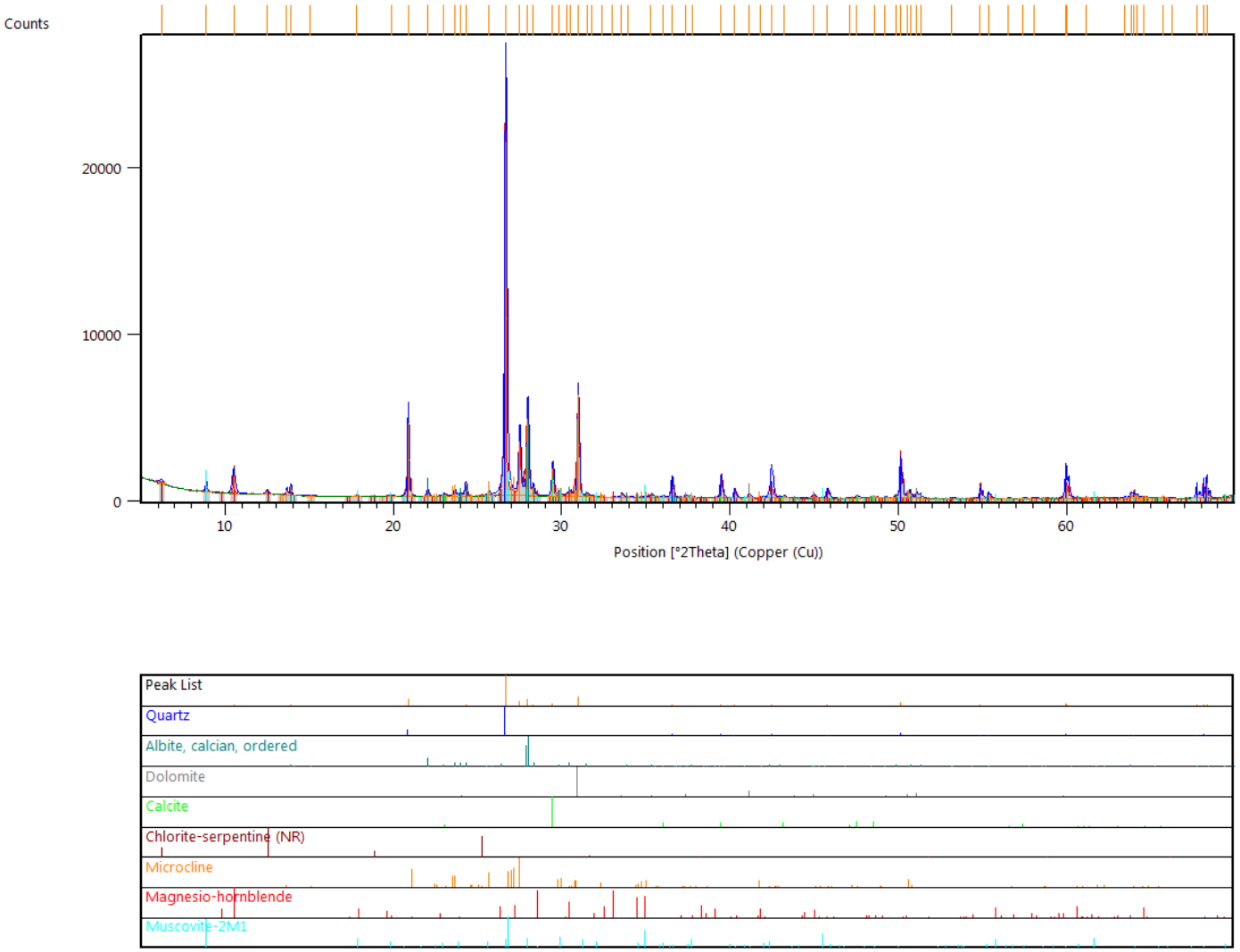

Figure 6. H002-8CS-3 phase ID.

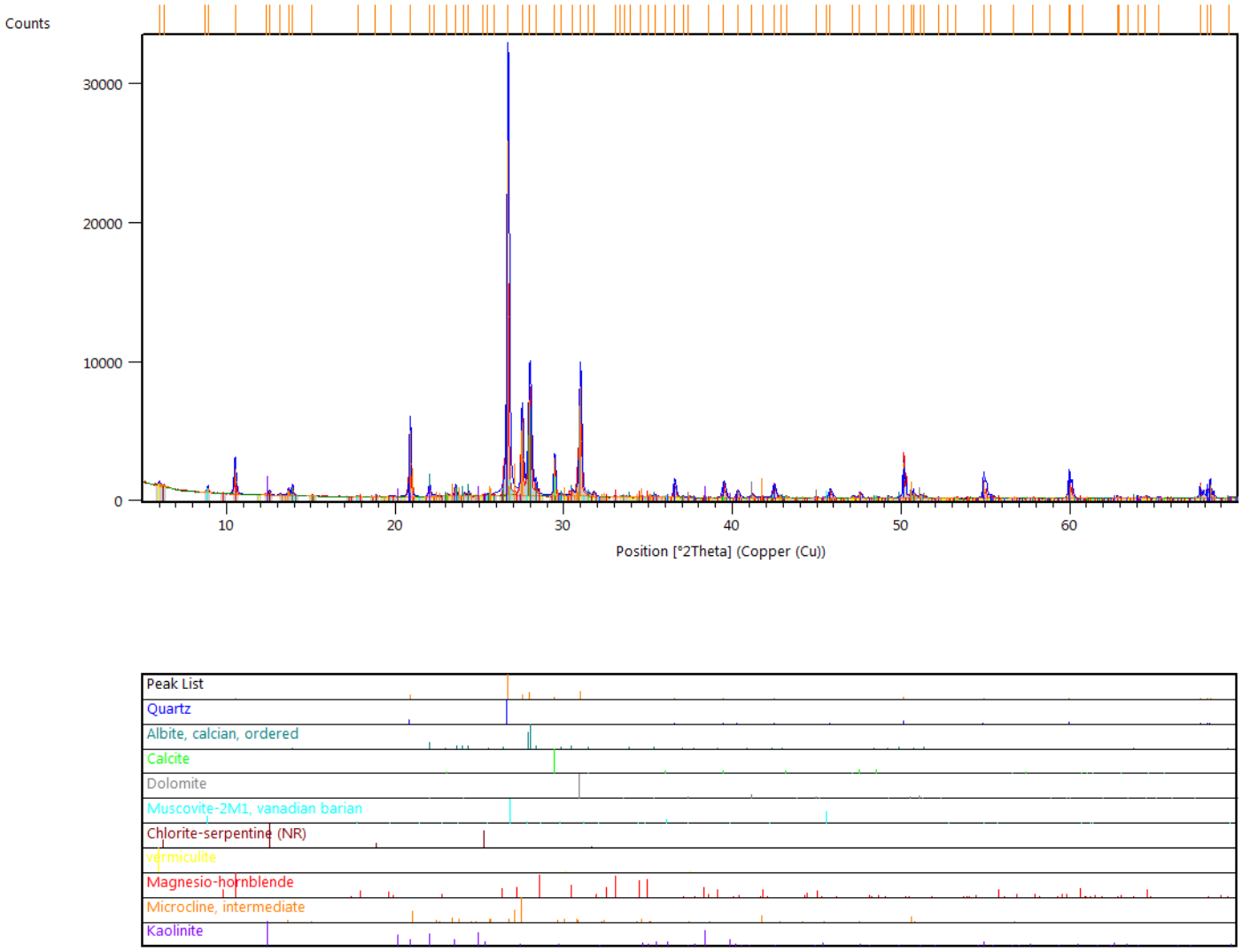

Figure 7. H002-12CS-3 phase ID (vermiculite is yellow).

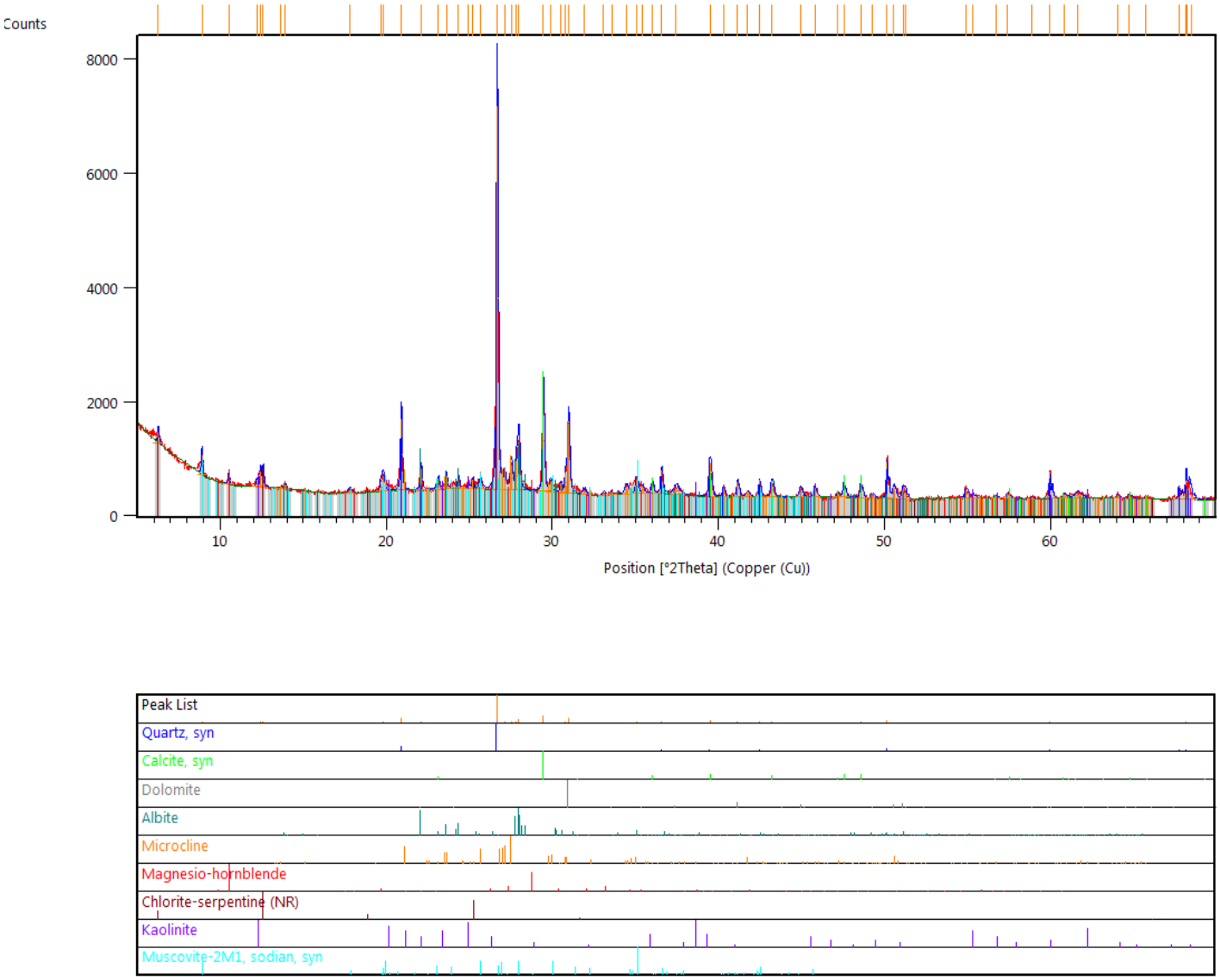

Figure 8. H005-1FB-1 phase ID.

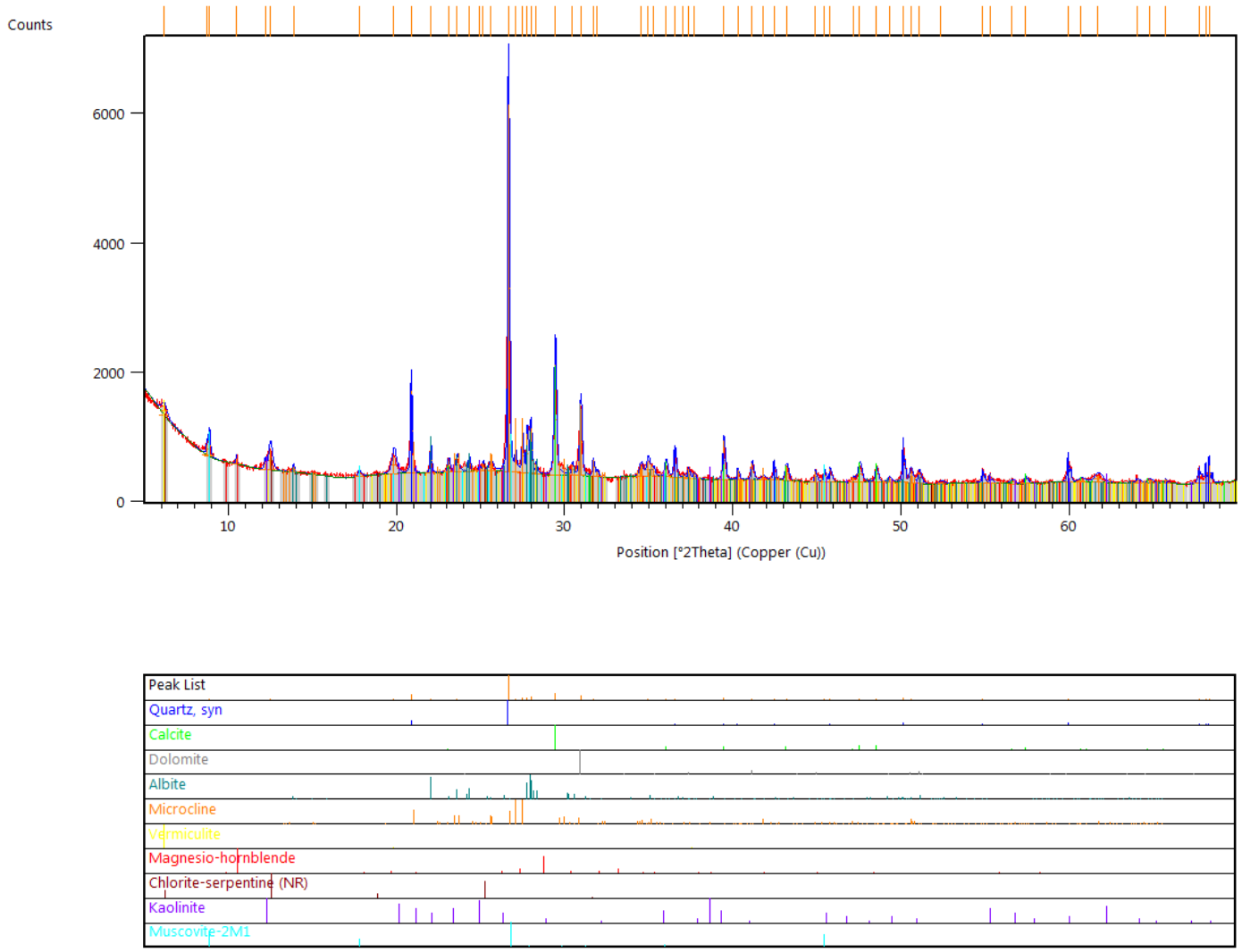

Figure 9. H005-1FB-2 phase ID (vermiculite is yellow).

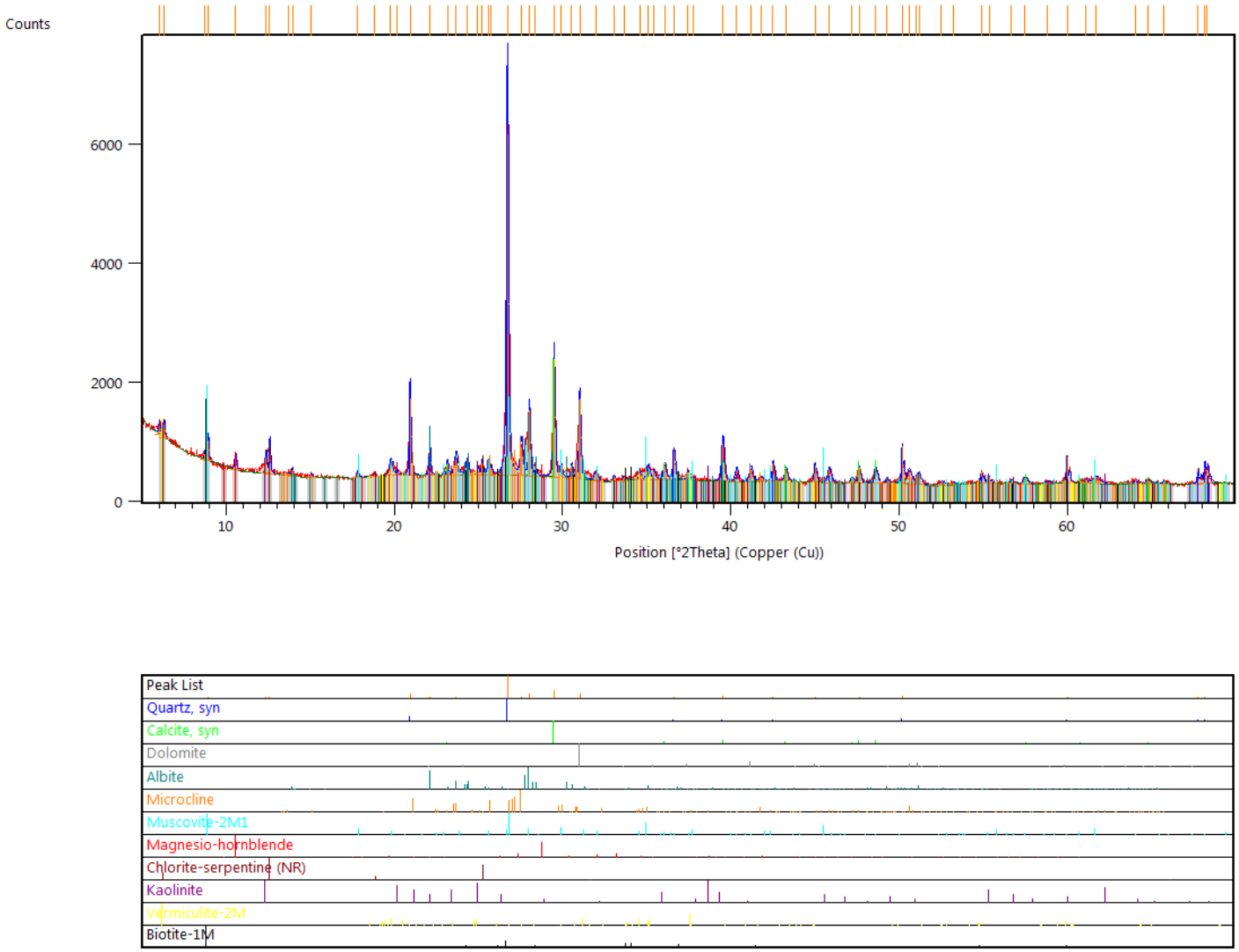

Figure 10. H005-1FB-3 phase ID (vermiculite is yellow).

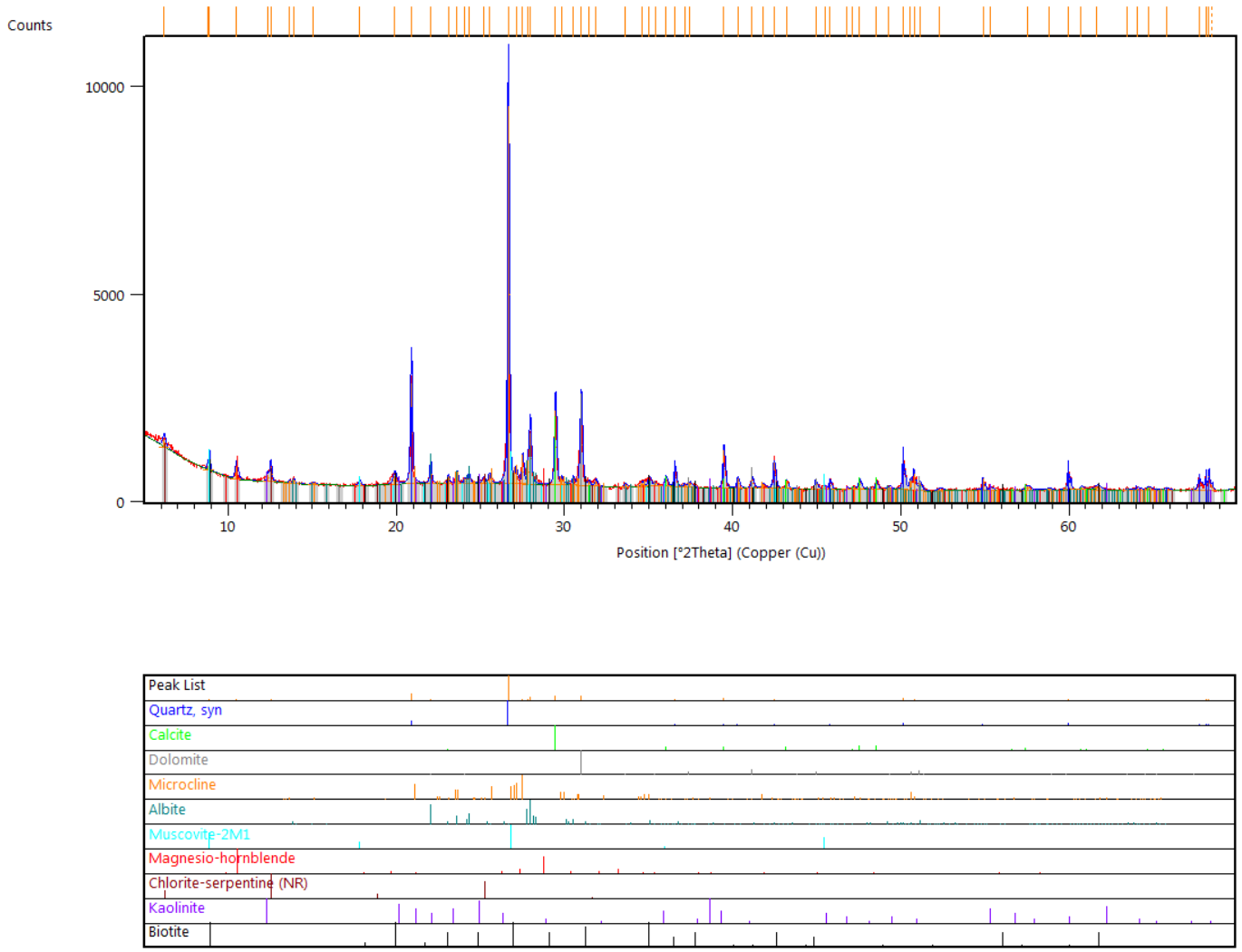

Figure 11. H005-2FB-1 phase ID.

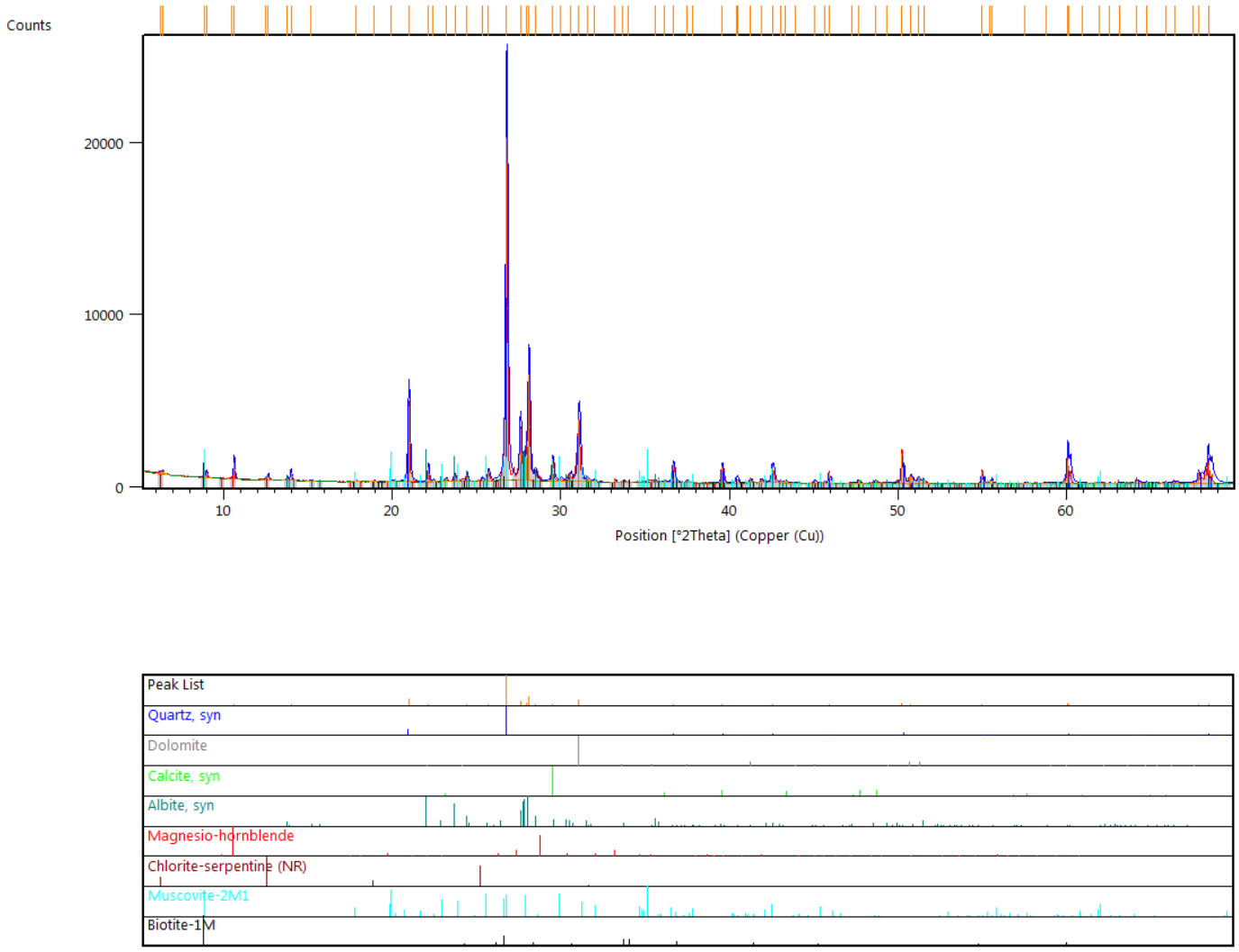

Figure 12. H005-3FB-3 phase ID.

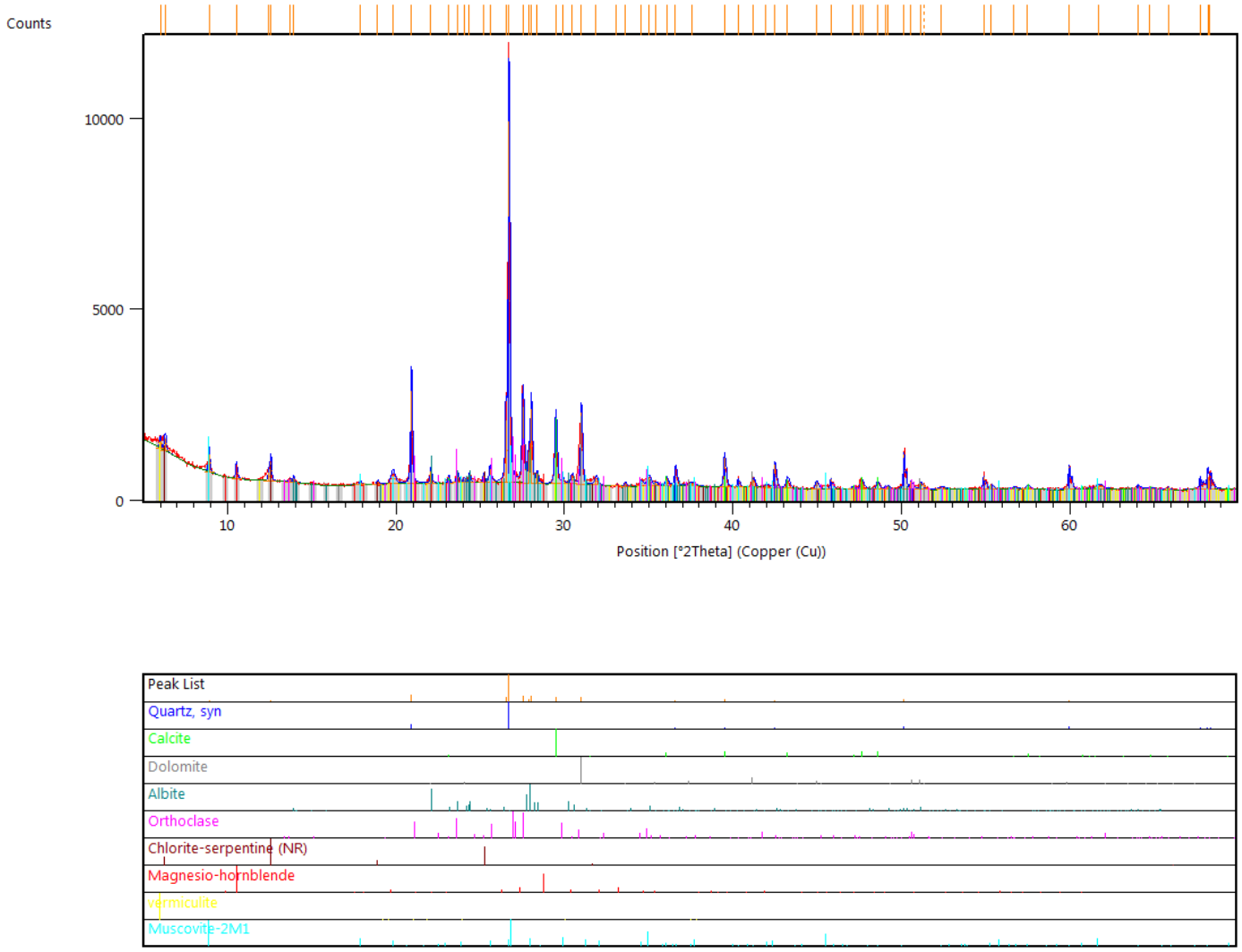

Figure 13. H005-4FB-3 phase ID (vermiculite is yellow).

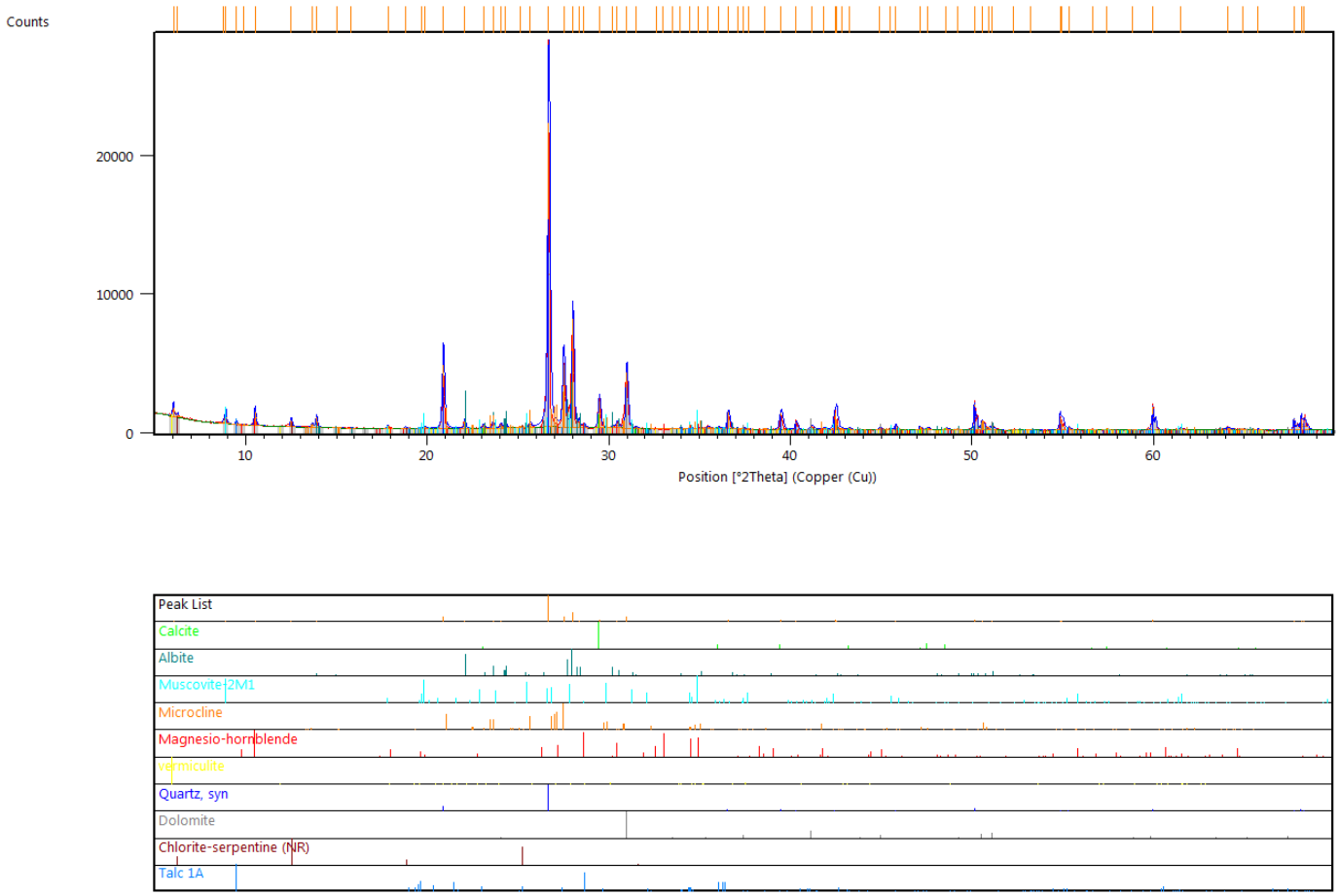

Figure 14. H005-4FB-4 phase ID (vermiculite is yellow).

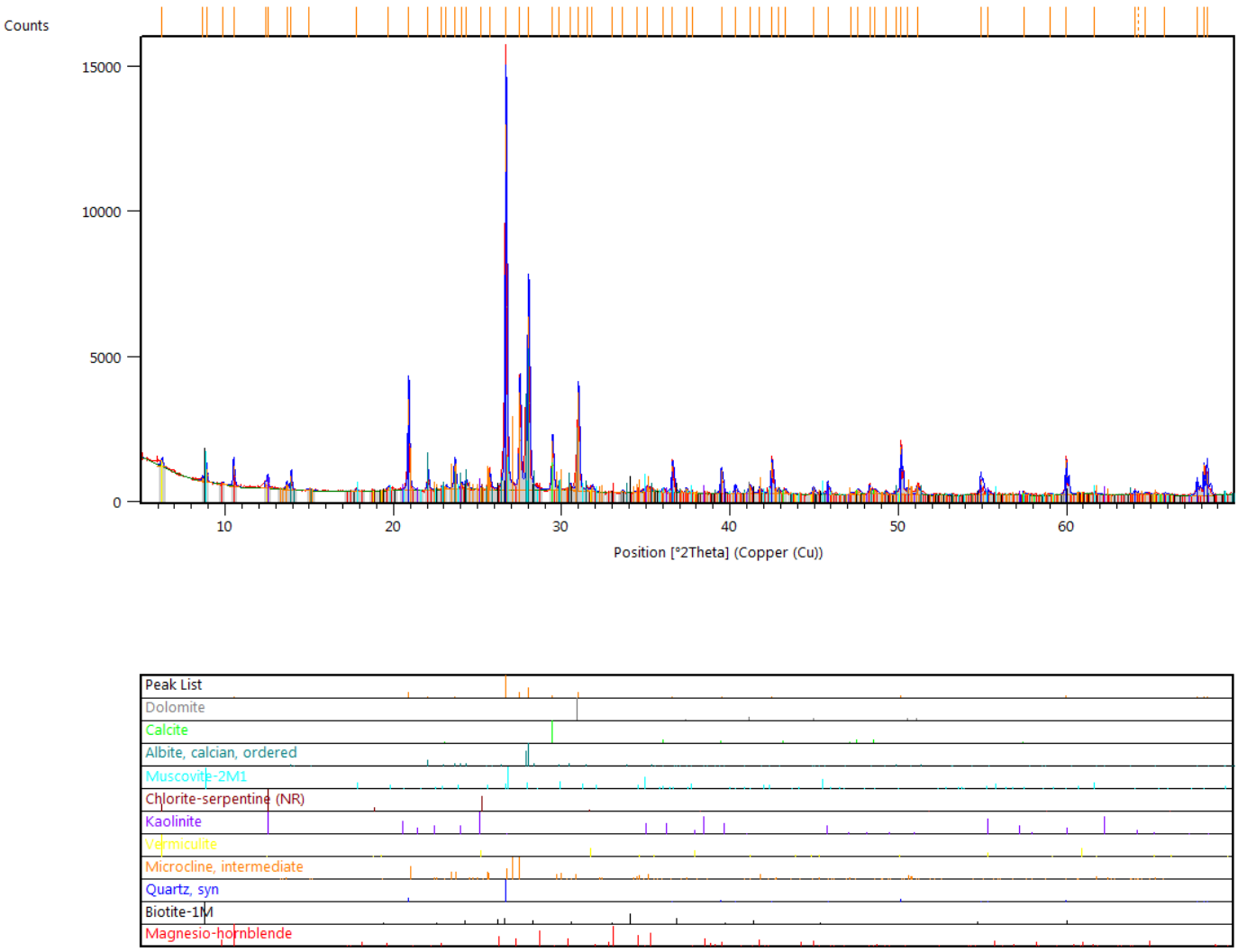

Figure 15. H005-9FB-1 phase ID (vermiculite is yellow).

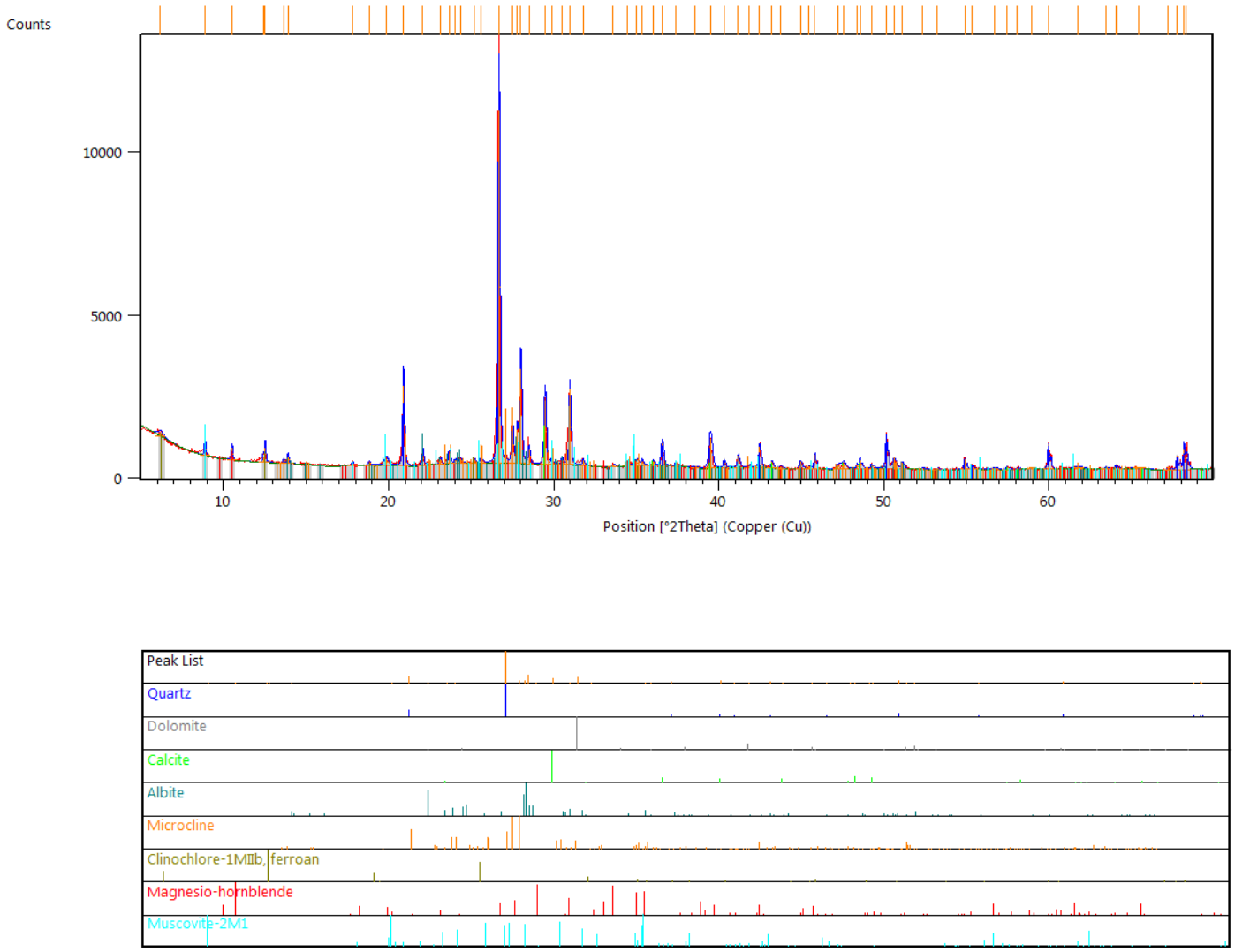

Figure 16. H005-9FB-4 phase ID.

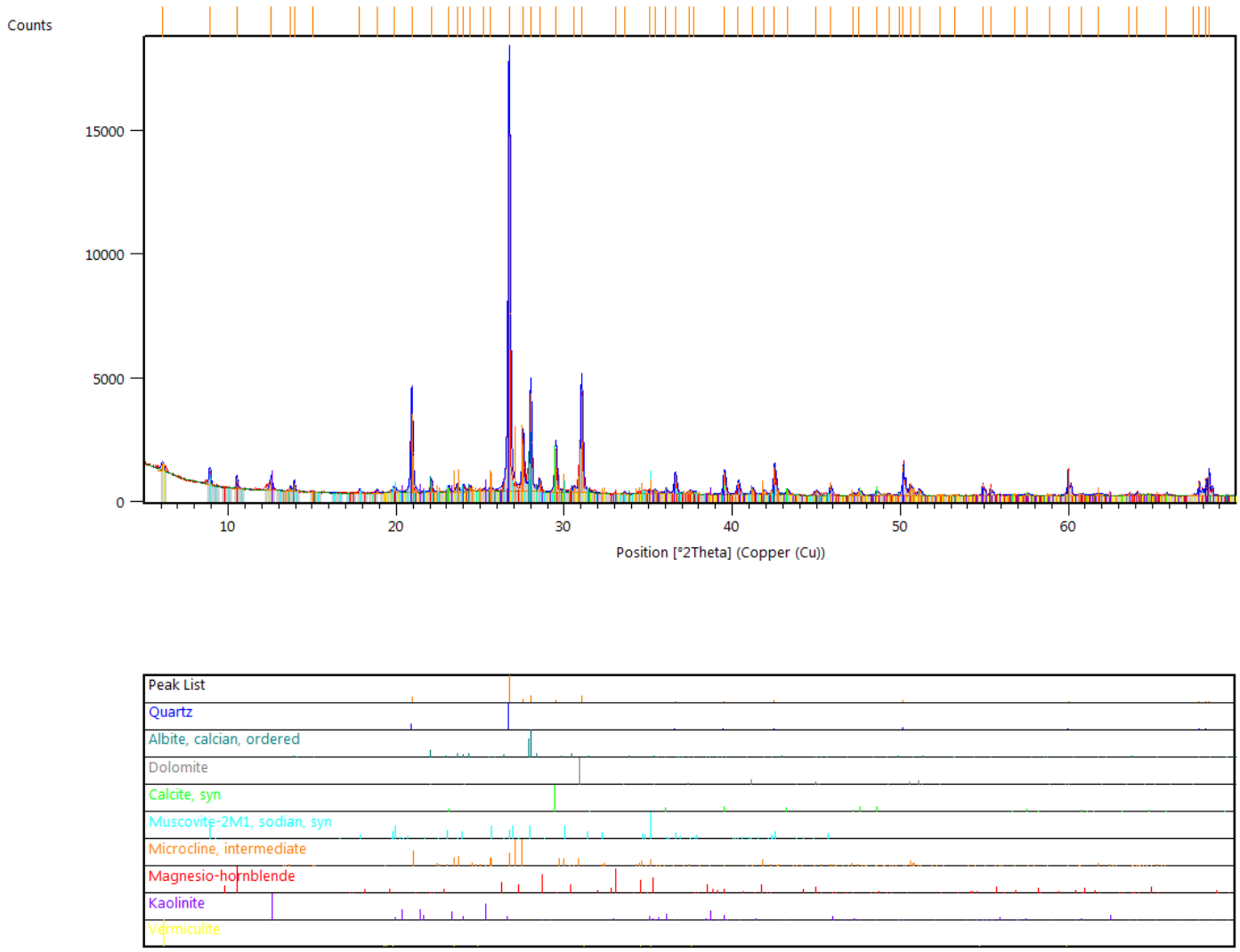

Figure 17. H005-9FB-4 phase ID (vermiculite is yellow).

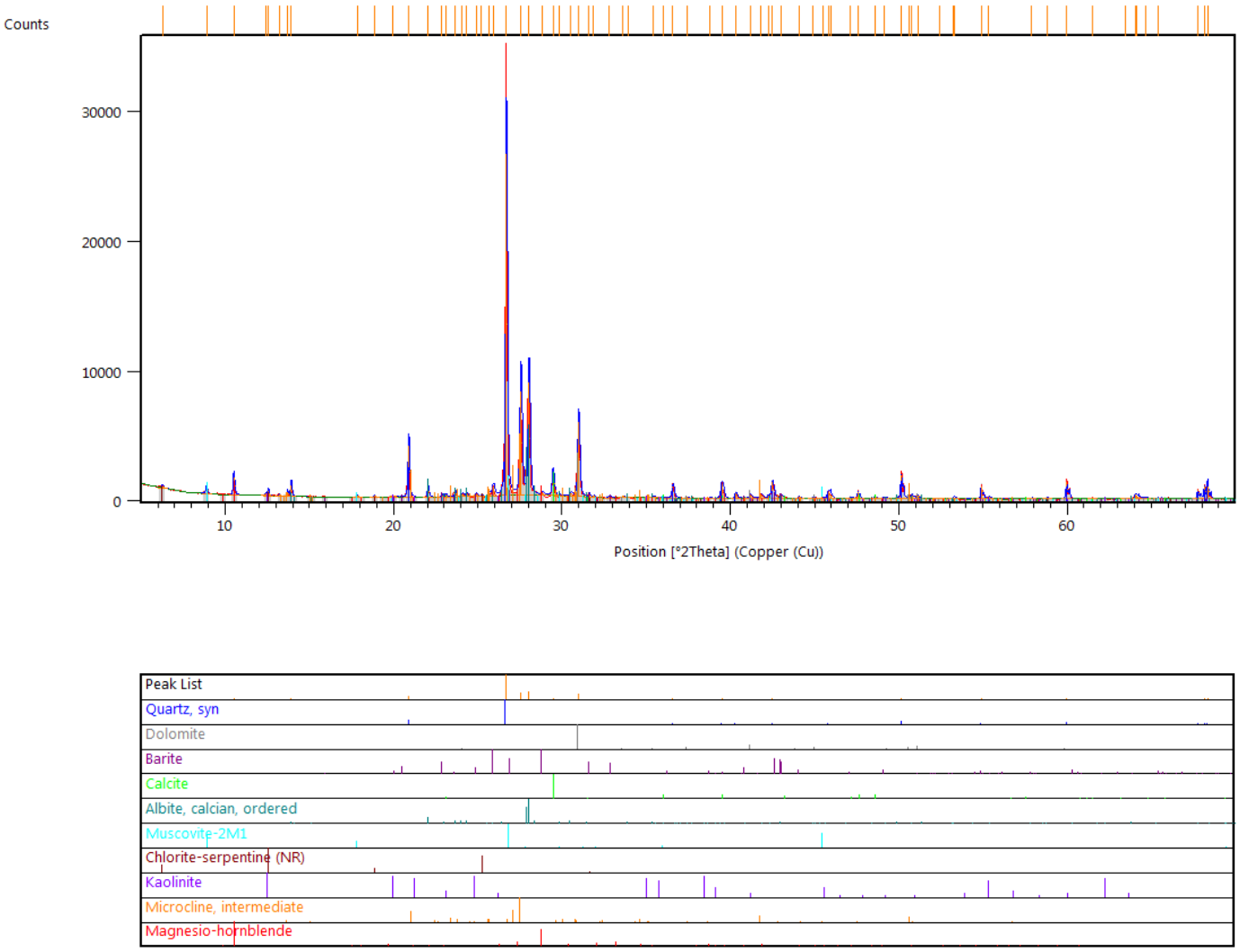

Figure 18. H005-12FB-3 phase ID.

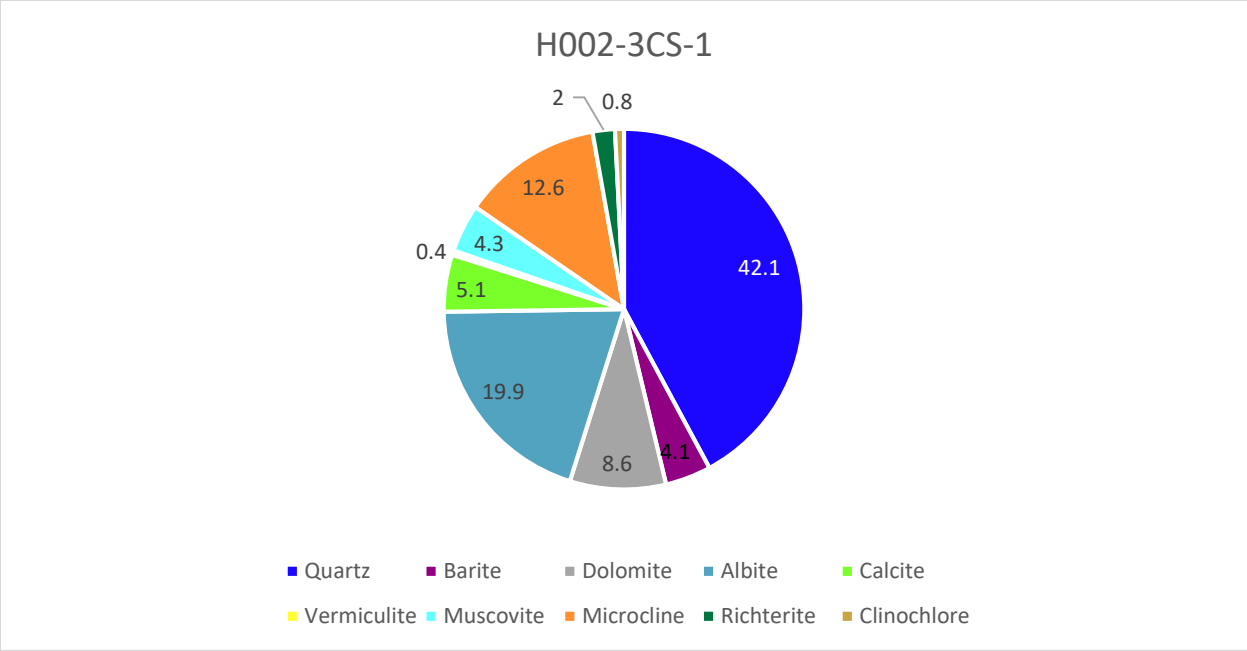

Figure 19. Rietveld refinement results of H002-3CS-1 (lithology type clayey-silt). The bulk results are shown in Figure 3. Numbers indicate weight percent.

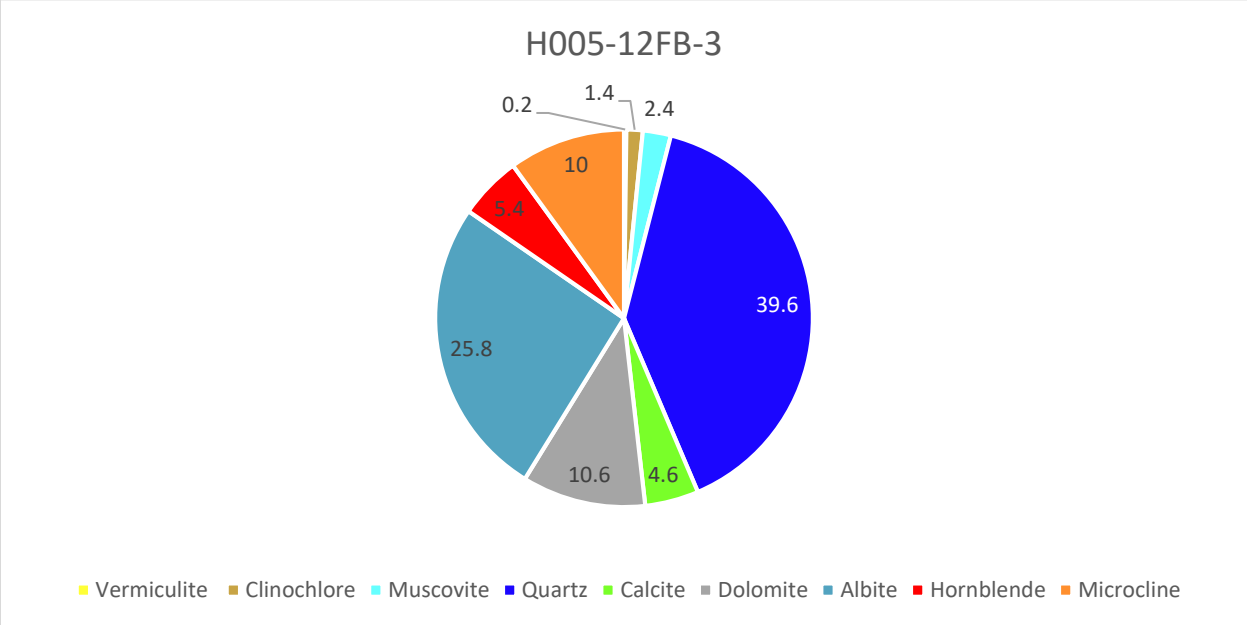

Figure 20. Rietveld refinement results of H005-12FB-3 (lithology type sandy silt). The bulk results are shown in Figure 18. Numbers indicate weight percent.

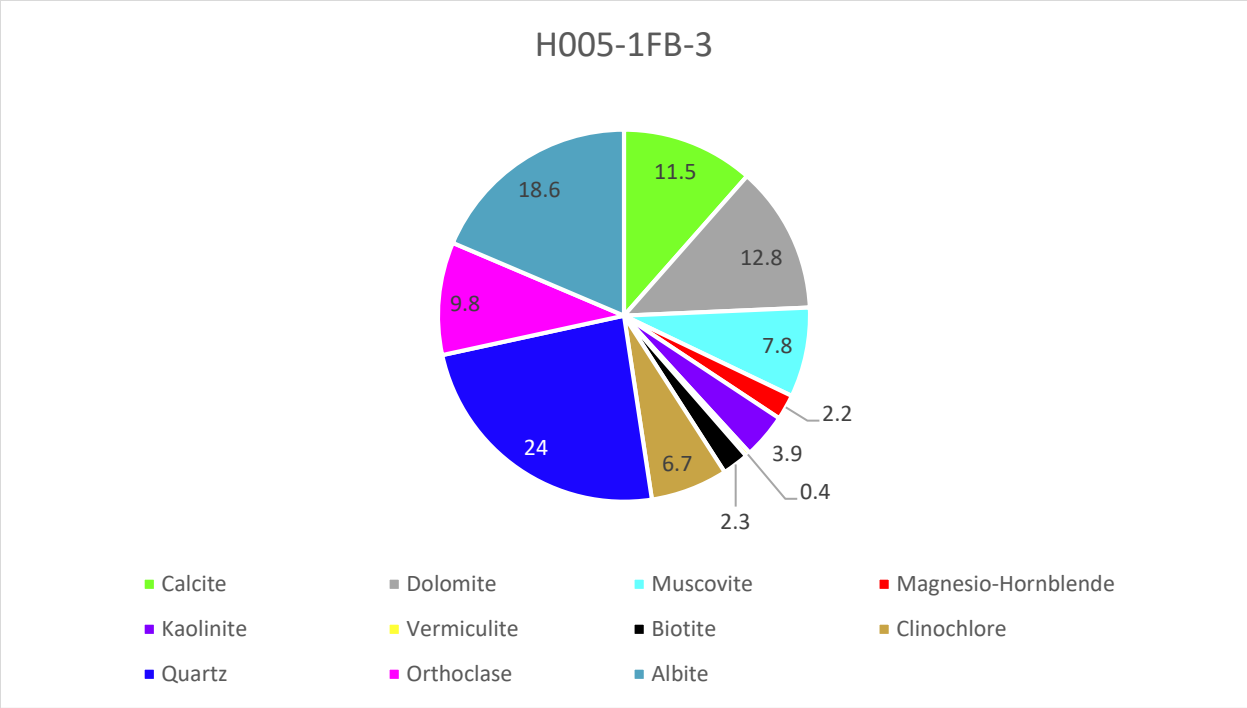

Figure 21. Rietveld refinement results of H005-1FB-3 (silty clay). The bulk results are shown in Figure 10. Numbers indicate weight percent.

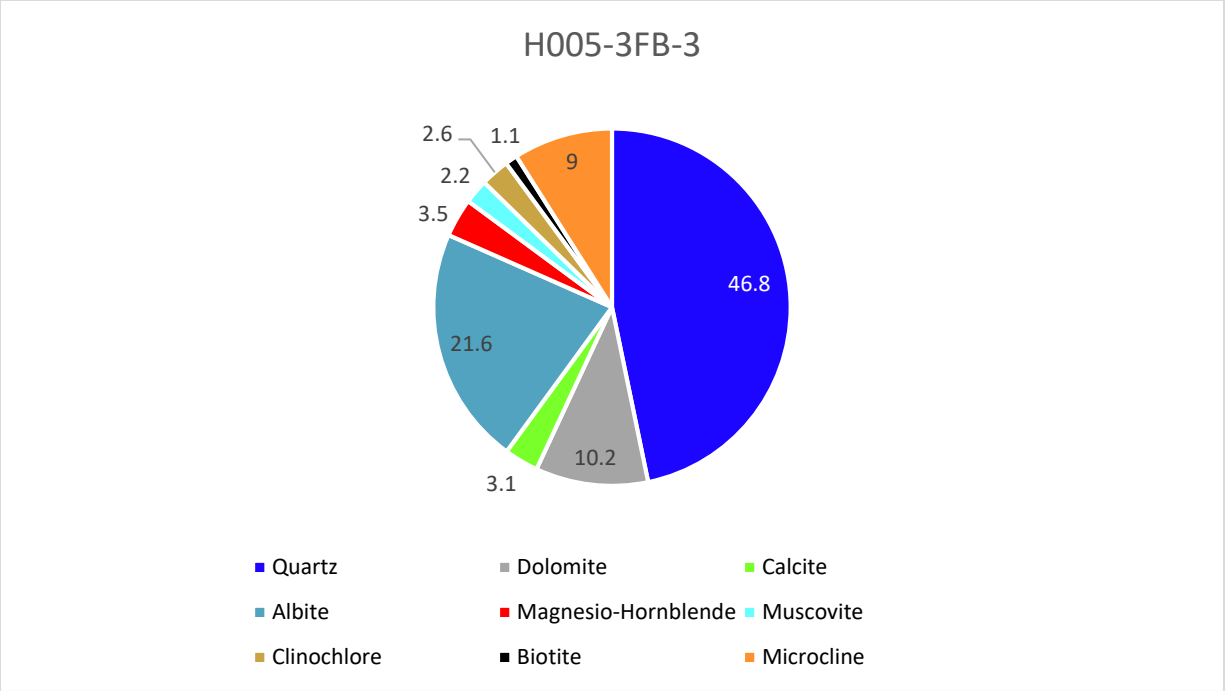

Figure 22. Rietveld refinement results of H005-3FB-3 (sandy silt). The bulk results are shown in Figure 12. Numbers indicate weight percent.

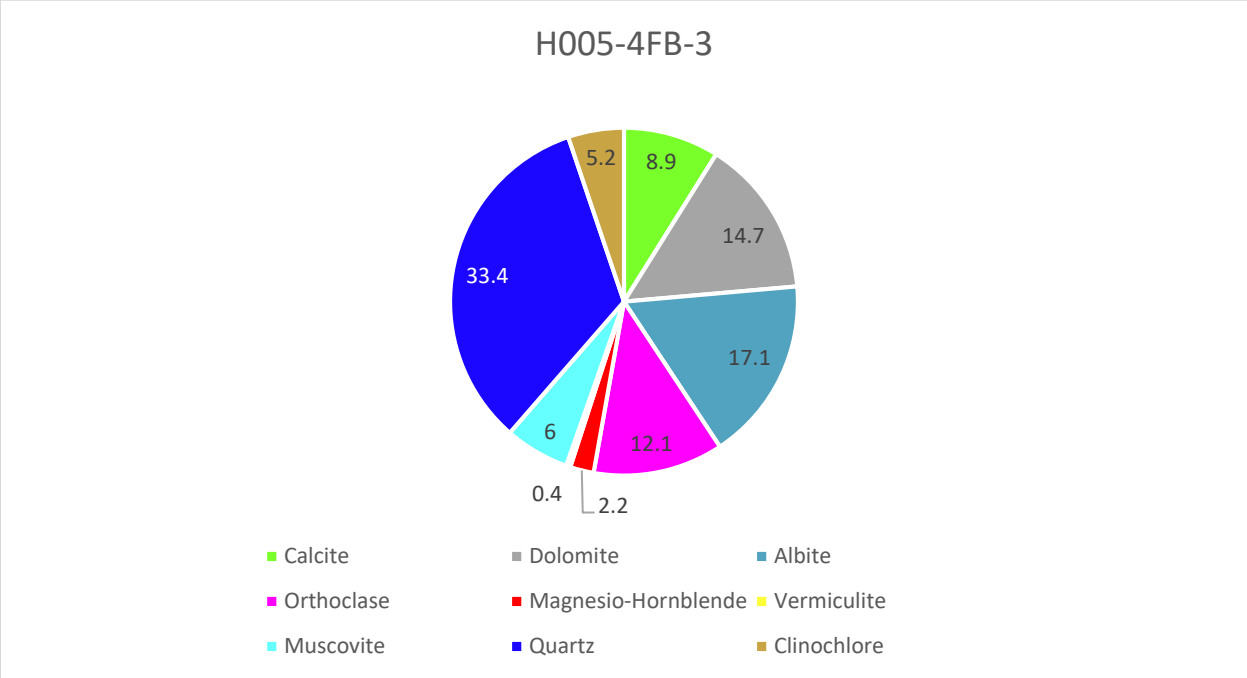

Figure 23. Rietveld refinement results of H005-4FB-3 (clayey silt). The bulk results are shown in Figure 13. Numbers indicate weight percent.

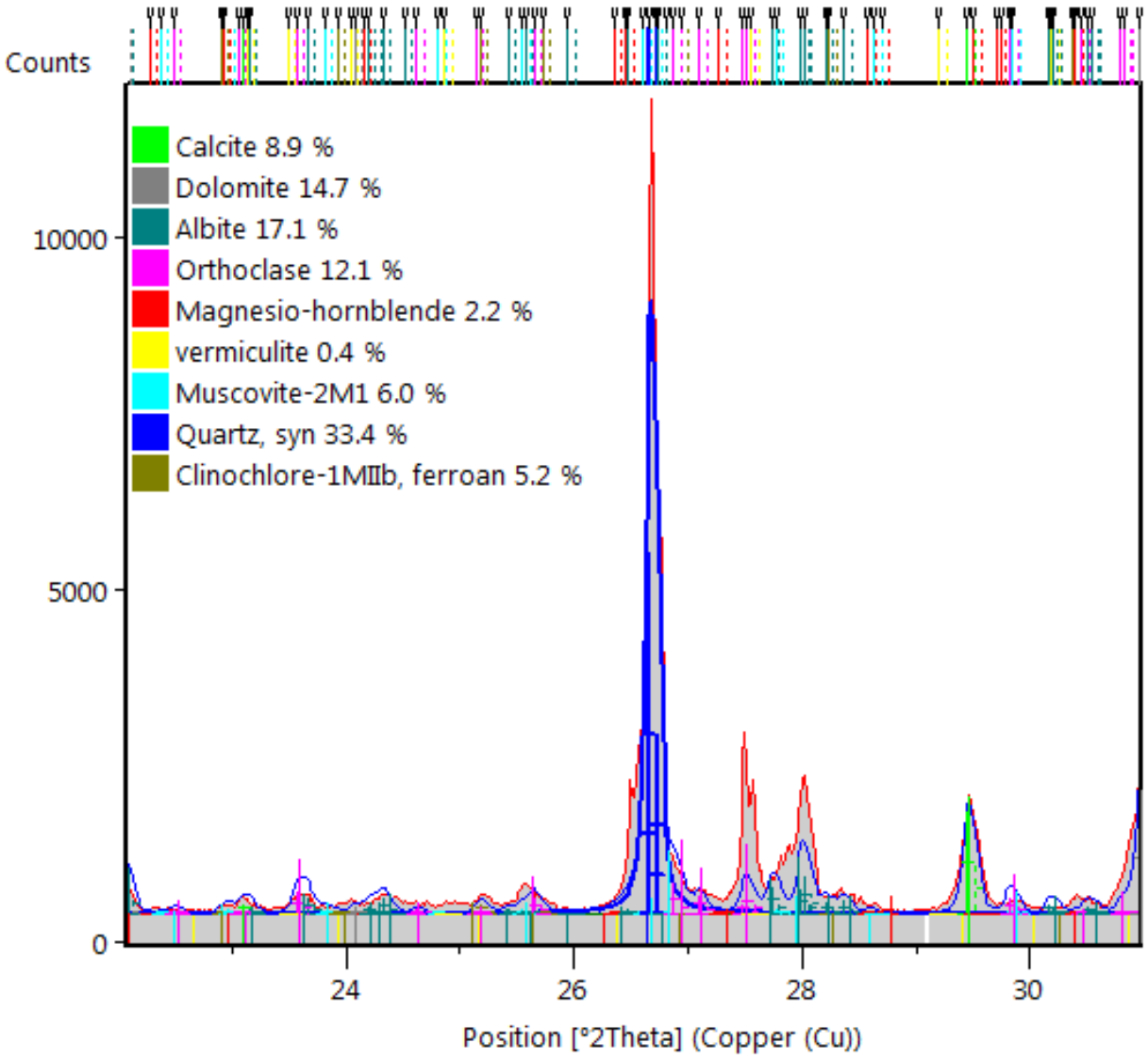

Figure 24. A calculated underestimation of a quartz peak (red) compared to its observed intensity (blue) from sample H005-4FB-3.

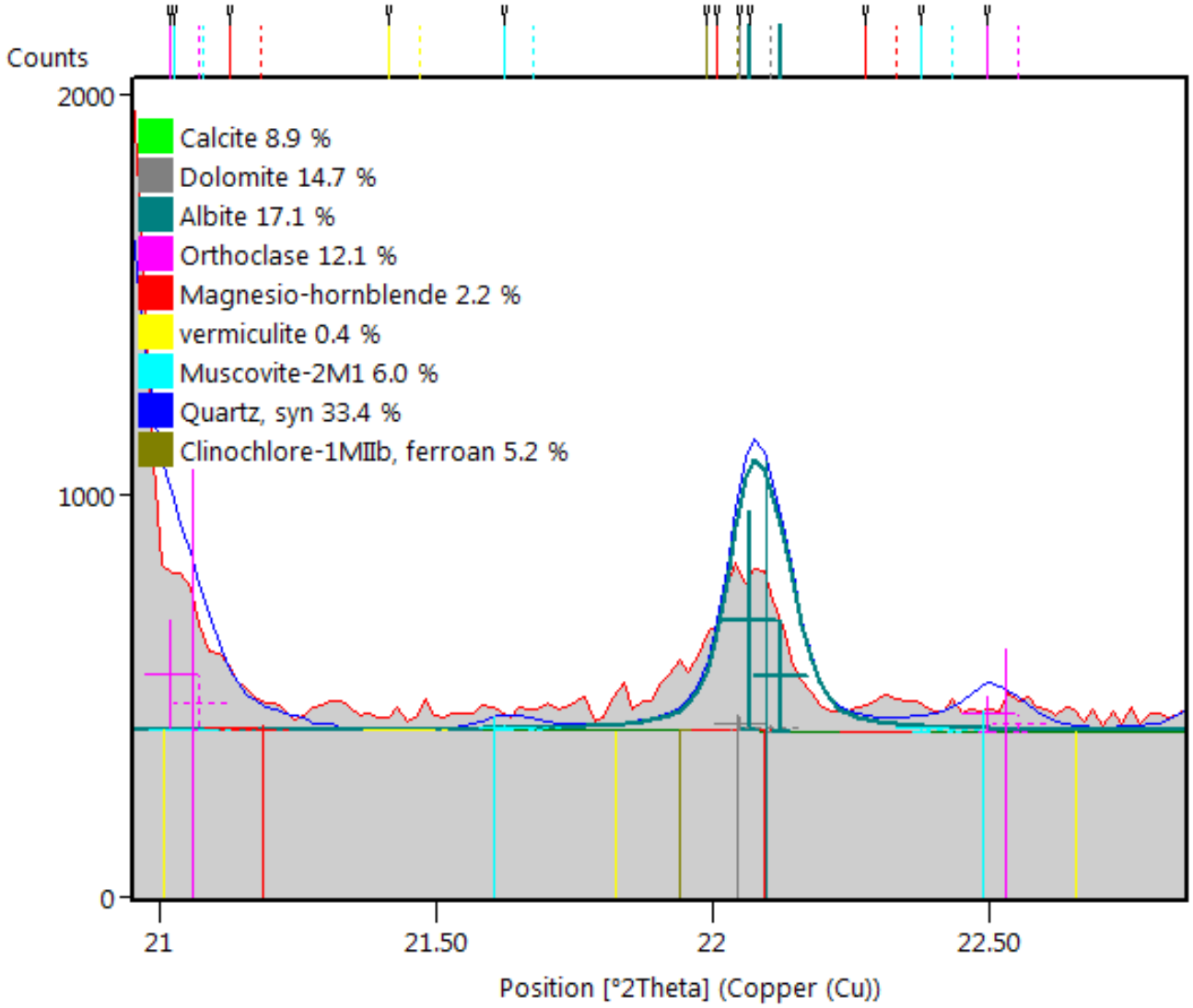

Figure 25. A calculated overestimation of an albite peak (red) compared to its observed intensity (blue) form sample H005-4FB-3.

7. Tables

Table 1. Subsamples taken from Ohio State cores after splitting or bagging. Note that the Interval column records the sample interval measured from the top of the core. However, in cases where the sediment was not in its original position due to incomplete core recovery or other core disturbance, it is not possible to know the true depth interval and have designated this as 'loose.'

Subsample	Lithology type (CS = clayey silt; SS = sandy silt)	Interval	Rietveld Analysis
H002-2CS-1	CS	Loose	
H002-3CS-1	SS	17-18cm	
H002-3CS-1	CS	16-24cm	Yes
H002-6CS-3	SS	Loose	
H002-7CS-1	CS	Loose	
H002-8CS-3	SS	Loose	
H005-9FB-1	CS	0-1cm	
H005-9FB-4	CS	0-7cm	
H005-12FB-3	SS	33-34cm	Yes
H005-12FB-3	CS	27-31cm	

Table 2. Subsamples sent to Ohio State University from the University of Texas from bagged degassing samples.

Subsample	Lithology type (CS = clayey silt; SS = sandy silt)	Interval	Rietveld Analysis
H005-1FB-1	Fall in material	0-69cm	
H005-1FB-2	Fall in material	69-163cm	
H005-1FB-3	SC	163-184cm	Yes
H005-2FB-1	Fall in material	0-18cm	
H005-3FB-3	SS	132.7-159.2cm	Yes
H005-4FB-3	CS	38.5-53.3cm	Yes
H005-4FB-4	SS	53.3-65cm	
H005-9FB-4	Multiple/uncertain	258-321cm	